

1-1-2022

Diagnostic accuracy of dual-energy CT to determine urinary tract stone composition: Differentiating between uric acid and non-uric acid urinary tract stone

Pawanaporn Rojanavijitkul

Pattama Tantigate

Supoj Ratchanon

Manint Usawachintachit

Krit Pongpirul

See next page for additional authors

Follow this and additional works at: <https://digital.car.chula.ac.th/clmjjournal>



Part of the [Medicine and Health Sciences Commons](#)

Recommended Citation

Rojanavijitkul, Pawanaporn; Tantigate, Pattama; Ratchanon, Supoj; Usawachintachit, Manint; Pongpirul, Krit; and Chaopathomkul, Bundit (2022) "Diagnostic accuracy of dual-energy CT to determine urinary tract stone composition: Differentiating between uric acid and non-uric acid urinary tract stone," *Chulalongkorn Medical Journal*: Vol. 66: Iss. 1, Article 10.

DOI: 10.14456/clmj.2022.10

Available at: <https://digital.car.chula.ac.th/clmjjournal/vol66/iss1/10>

This Article is brought to you for free and open access by the Chulalongkorn Journal Online (CUJO) at Chula Digital Collections. It has been accepted for inclusion in Chulalongkorn Medical Journal by an authorized editor of Chula Digital Collections. For more information, please contact ChulaDC@car.chula.ac.th.

Diagnostic accuracy of dual-energy CT to determine urinary tract stone composition: Differentiating between uric acid and non-uric acid urinary tract stone

Authors

Pawanaporn Rojanavijitkul, Pattama Tantigate, Supoj Ratchanon, Manint Usawachintachit, Krit Pongpirul, and Bundit Chaopathomkul

Original article

Diagnostic accuracy of dual-energy CT to determine urinary tract stone composition: Differentiating between uric acid and non-uric acid urinary tract stone

Pawanaporn Rojanavijitkul^a, Pattama Tantigate^a, Supoj Ratchanon^b, Manint Usawachintachit^b, Krit Pongpirul^c, Bundit Chaopathomkul^{a,*}

^a Department of Radiology, Faculty of Medicine, Chulalongkorn University, and King Chulalongkorn Memorial Hospital, The Thai Red Cross Society, Bangkok, Thailand

^b Department of Surgery, Faculty of Medicine, Chulalongkorn University, Bangkok, Thailand

^c Department of Preventive and Social Medicine, Faculty of Medicine, Chulalongkorn University, Bangkok, Thailand

Background: The urinary tract stone is a worldwide condition with various clinical significances. Optimal treatment requires multiple considerations including stone composition. Dual-energy computed tomography (DECT) has been used to determine uric acid and non-uric acid urinary tract stones.

Objective: To evaluate the diagnostic accuracy of rapid-kilovoltage (kV) switching DECT in differentiating between uric acid and non-uric acid stones compared with reference standard infrared spectroscopy (IRS).

Methods: A prospective study enrolled patients from February 2018 to March 2020 who underwent a DECT scan for urinary tract stone with ≥ 3 -mm stone (s). Post-processed material-density (MD) images were used to differentiate between uric acid and non-uric acid stones. Exclusion criteria included those with no available IRS result or those with an unclear location of the extracted stone on CT images. Diagnostic accuracy was analyzed using SPSS® v.22.

Results: A total of 28 patients with 35 urinary tract stones were included composing of 2 uric acid and 33 non-uric acid stones. There were 50.0% sensitivity, 96.8% specificity, 50.0% positive predictive value (PPV), 96.8% negative predictive value (NPV) and 93.9% accuracy of MD images compared to IRS.

Conclusion: Rapid-kV switching DECT has high accuracy to determine non-uric acid stones.

Keywords: Material density images, dual-energy CT, urinary tract stone, uric stone, rapid kilovoltage (kV) switching.

The urinary tract stone is a common worldwide condition associated with multiple genetic and environmental factors with a high recurrence rate over 60.0 – 80.0% during a lifetime.⁽¹⁾ The prevalence ranged from 7.0 – 13.0% in North America, 5.0 – 9.0% in Europe, 1.0 – 19.1% in Asia and up to 16.9% in Thailand especially in the Northeast region.⁽¹⁻³⁾ In Asia, the most common composition

of the urinary tract stones was calcium oxalate 75.0 – 90.0%, followed by uric acid 5.0 – 20.0%.⁽¹⁾ Clinical manifestations are varying from subclinical symptoms to life-threatening conditions, raising the importance of its proper management. Apart from the stone size and location, the stone composition was also considered to determine specific management, success rate, and recurrence rate.⁽⁴⁾ For example, small stones could pass spontaneously with clinical observation. Moreover, uric acid stones could be medically treated with urine alkalinization, while calcium-containing stones usually required surgical intervention.⁽⁴⁾

Conventional non contrast-enhanced computed tomography (NECT) is the diagnostic imaging modality of choice. Conventional NECT provides

*Correspondence to: Bundit Chaopathomkul, Department of Radiology, Faculty of Medicine, Chulalongkorn University, and King Chulalongkorn Memorial Hospital, The Thai Red Cross Society, Bangkok 10330, Thailand
E-mail: bchaopathomkul@gmail.com

Received: December 16, 2020

Revised: February 10, 2021

Accepted: March 9, 2021

accurate size, location, attenuation, and also established complications. The stone attenuation, reported in the Hounsfield unit (HU), has been used to determine its composition; however, there are still some pitfalls especially in those with a size less than millimeters.⁽⁴⁻⁶⁾

Dual-energy computed tomography (DECT) has been increasingly used to determine stone composition, mainly to differentiate uric acid stone from non-uric acid stone.⁽⁷⁾ Most published studies have used dual-source DECT while rapid-kilovoltage (kV) switching DECT has scarcely been reported.⁽⁸⁻¹⁰⁾ In the range of diagnostic X-ray spectrum, two main photon-matter interactions occurred: Compton and Photoelectric effects. The Compton effect or Compton scattering depends on outer shell electron density while the Photoelectric effect, which is responsible for diagnostic image generation, strongly depends on the atomic number.⁽¹¹⁾ With material decomposition algorithm or material-density (MD) images postprocessed from rapid-kV switching DECT, materials with high atomic number (iodine) and low atomic number (water) can be differentiated.⁽⁶⁾

The purpose of this study was to evaluate the diagnostic accuracy of rapid-kV switching DECT to differentiate between uric acid and non-uric acid stones using MD images, comparing with reference standard infrared spectroscopy (IRS).^(4, 12) The secondary outcome was to evaluate radiation dose from rapid-kV switching DECT.

Materials and methods

Patient selection

The prospective study has been approved by the institutional review board and written informed consents were obtained from all participants. We enrolled ≥ 18 -year-old patients who were scheduled for a CT scan for urinary tract stone from February 2018 to March 2020. All patients underwent a CT scan followed by stone extraction for stone analysis using the IRS. Those with urinary tract stone(s) sized less than 3 millimeters or unclear extracted stone location on CT images were excluded. Data of stone location was obtained from medical records, operative notes, and follow-up imaging. Those with a single urinary tract stone, stones with exact locations written on operative notes, and stones that disappeared on the follow-up imaging, were finally counted for statistical analysis. A total of 173 patients were enrolled and, finally, stones from 28 patients were included and analyzed.

The study has been approved by the Ethical Committees, the Institutional Review Board, Faculty of Medicine, Chulalongkorn University, Bangkok, Thailand. (IRB no. 675/60).

Scanning protocol and Image postprocessing

The scans were obtained by using a 64-slice rapid-kV switching DECT (Discovery CT 750 HDCT, GE Healthcare, Milwaukee, WI). The patients were non-fasting, lying in the supine position, arms over their heads and scanned for two consecutive image acquisitions. First, conventional NECT axial helical scan of the whole abdomen was performed to confirm the existence of the urinary tract stone(s). The parameters included 120 kVp, automated tube current modulation (ATCM) within range of 100 - 650 mA, slice thickness 2.5 mm, gantry rotation time 0.5 second, pitch 1.375, and detector coverage 64 x 0.625 mm. The images were reconstructed with adaptive statistical iterative reconstruction (ASIR) algorithm using 50.0% ASIR, receiving axial images (2.5-mm slice thickness, 1-mm interval), and then reformatted into coronal and sagittal images (5-mm slice thickness and 3-mm interval).

Second, rapid-kV switching DECT axial helical scan was performed over areas of urinary tract stone(s) using rapid switching of 80/140 kVp in less than 0.5 msec.

The mA and gantry rotation time were automatically adjusted to optimize radiation dose and image quality. All data were sent to the vendor's specific commercial workstation (ADW version 4.6; GE Healthcare) for postprocessing image reconstruction. Material-density (MD) images were performed by using a pair of water and iodine images to differentiate uric acid from non-uric acid stones.⁽⁶⁾

Image analysis

The images were reviewed with the consensus of an experienced abdominal radiologist and a diagnostic radiology resident. On conventional 120 kVp NECT images, number, location, size, and attenuation of all ≥ 3 -mm stones were recorded. Two material decomposition algorithm or MD images (water and iodine images) was used to determine uric acid and non-uric acid stone.⁽⁶⁾ The stones presented on water but not iodine images were categorized as "uric acid stones", while those presented on both water and iodine images were categorized as "non-uric acid stones".

Radiation dose analysis

The volume computed tomography dose index (CTDI_{vol}, mGy) and dose-length product (DLP, mGy-cm) from conventional NECT for whole abdomen and DECT for the area of urinary tract stone was recorded. Effective radiation dose (mSv) from each scan was calculated by multiplying DLP with 0.015 (effective factor for CT abdomen and pelvis).

Infrared spectroscopy (IRS)

According to reference standard IRS, all extracted stones with clear locations on CT images were analyzed using Thermo Scientific™ Nicolet™ Spectrometer with iS50 FTIR or iS5 FTIR generation.⁽¹²⁾ Pure or near-pure stone was defined as at least 80.0% of one major component.⁽¹³⁾

Statistical analysis

All statistical analyses were performed using SPSS® v.22 (IBM Corp., New York, NY; formerly SPSS Inc., Chicago, IL). Descriptive analysis was performed and reported in percentages, median with range, and mean ± SD. Analysis for diagnostic

accuracy of MD images compared with IRS was reported in terms of sensitivity, specificity, positive predictive value (PPV), negative predictive value (NPV) and accuracy, each with 95.0% confidence interval (CI). Interrater agreement was reported in term of Cohen’s Kappa statistic (less than 0: poor agreement; 0.00 – 0.20: slight agreement; 0.21 – 0.40: fair agreement; 0.41 - 0.60: moderate agreement; 0.61 – 0.80: substantial agreement; and, 0.81 – 1.00: almost perfect agreement).

Results

A total of 173 patients were enrolled; and, finally, 28 patients with 35 stones were analyzed. There were 13 males and 15 females with mean age of 60.0 ± 16.0 years old (range 29 - 88 years old). Median of stone diameter was 0.9 cm (range 0.3 - 7.5 cm). The stone locations were listed in descending order of frequency: ureters (45.7%), calyces (28.6%), renal pelvis (14.3%), and, equally, ureteropelvic junction (UPJ) (2.9%), ureterovesicular junction (UVJ) (2.9%), bladder (2.9%), and urethra (2.9%).

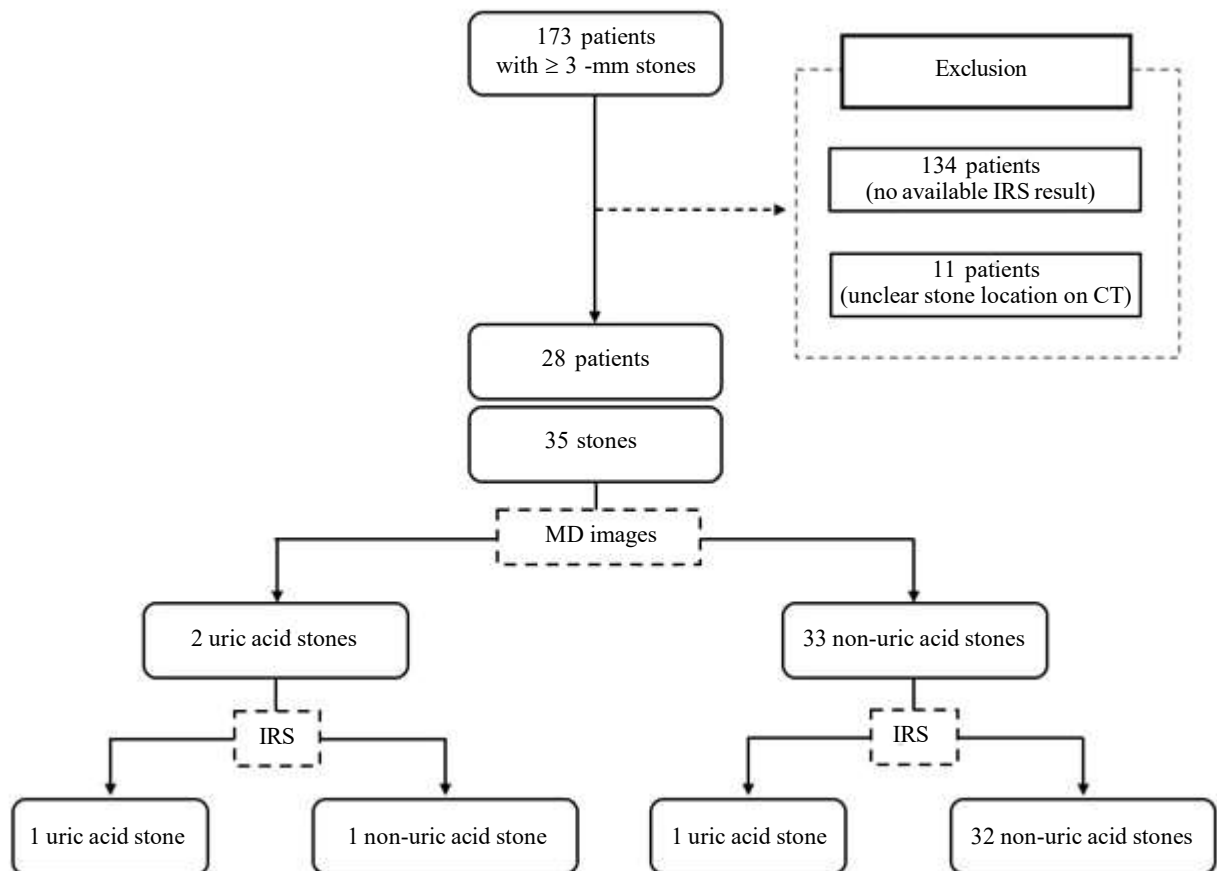


Figure 1. Case selection procedure and categorization (MD images = material-density images; IRS = Infrared spectroscopy).

By MD images, 2 uric acid stones and 33 non-uric acid stones were recorded (Figure 1). Mean attenuations in the Hounsfield unit (HU) calculated on conventional 120 kVp NECT images were 576.5 ± 9.2 HU (range 570 - 583 HU) for uric acid stones and 804.8 ± 381.0 HU (range 160 - 1,464 HU) for non-uric acid stones. Of these 2 uric acid stones, one had been confirmed to be a pure uric acid stone by standard IRS (true positive result, Figure 2) while the other one turned out to be a non-uric acid stone (false positive result, Figure 3). In 33 non-uric acid stones, 32 stones had been confirmed to be pure or predominantly non-uric acid stones (true negative result, Figure 4), while the other one turned out to be a pure uric acid stone (false negative result, Figure 5). Analysis of diagnostic accuracy showed sensitivity of 50.0% (95%CI; 1.26 - 98.74), specificity of 96.8% (95%CI; 84.20 - 99.92), positive predictive value (PPV) of 50.0% (95%CI; 1.26 - 98.74), negative

predictive value (NPV) of 96.8% (95%CI; 84.20 - 99.92) and accuracy of 94.3% (95%CI; 80.84 - 99.30) (Table 1). Cohen's Kappa statistic was 0.47, referring to a moderate agreement between MD images and the IRS.

As for radiation exposure, mean $CTDI_{vol}$ (mGy), DLP (mGy·cm) and effective radiation dose (mSv) were 9.9 ± 3.6 , 536.2 ± 222.0 and 8.0 ± 3.3 for conventional NECT of the whole abdomen, and 11.2 ± 2.7 , 323.9 ± 161.3 , and 4.9 ± 2.4 for DECT of the area of urinary tract stone(s). Mean total individual effective radiation dose was 12.9 ± 5.0 mSv. Mean percentage of DECT scan length as compared to 100.0% of NECT was $47.3 \pm 20.2\%$ (range 16.4 - 87.9%). The effective radiation dose from DECT calculated to 100.0% scan length (equal to NECT for the whole abdomen) was 10.5 ± 3.6 mSv or about 130.6% as compared to NECT.

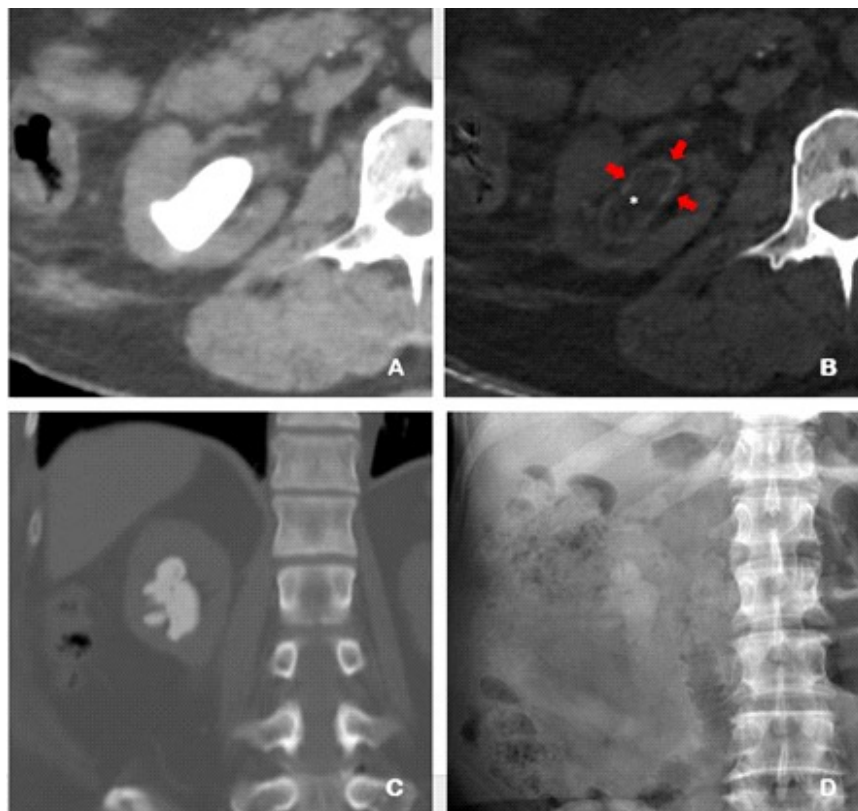


Figure 2. CT images and plain KUB radiograph of a true positive stone. MD, water (A) and iodine (B), images showed a staghorn stone in right kidney, with predominantly uric acid component (*) in the central part surrounded with a thin peripheral non-uric acid component (red arrows). IRS revealed a pure uric acid component. Coronal-reformatted NECT images (C) showed heterogeneously high density of the stone, about 570 HU, along with a radio-opaque stone seen on plain KUB radiograph (D), suggestive of some degree of non-uric acid component.^(5, 6, 14) These might be explained by sampling error of the IRS due to stone fragmentation from percutaneous nephrolithotomy (PCNL).

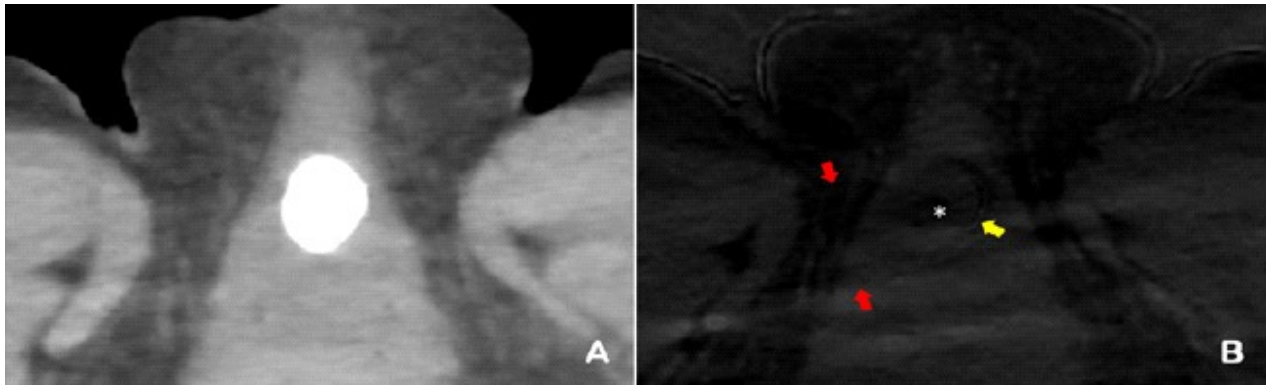


Figure 3. MD images of a false positive urethral stone. A predominantly uric acid stone seen on water (A) but hardly seen on iodine (B) images. Majority of uric acid component at its central part was demonstrated (*). A thin curvilinear non-uric acid component at periphery was also present (yellow arrow). IRS revealed majority of non-uric acid (Dahllite) component. A large crossing streak artifact (red arrow) from pelvic bone over the field of view was found.

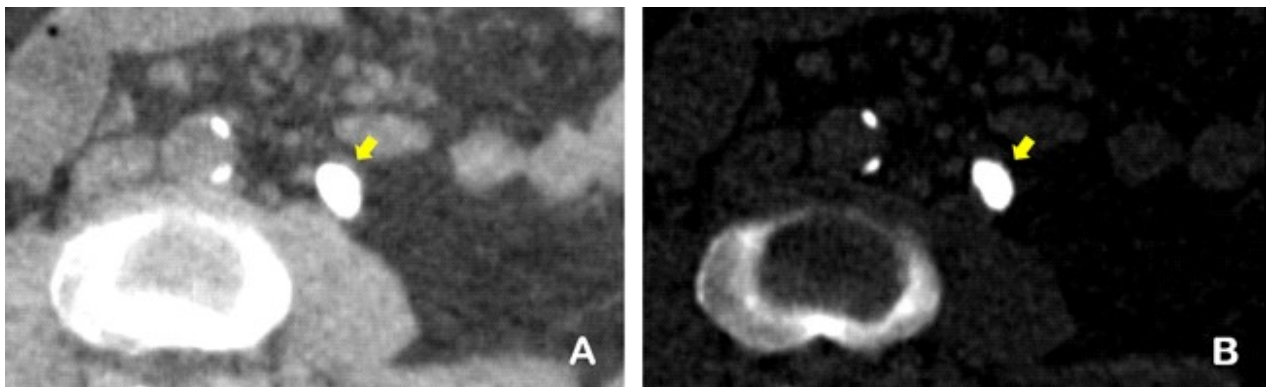


Figure 4. MD images of a true negative stone. The images showed a non-uric acid left ureteric stone presented on both water (A) and iodine (B) images. IRS revealed a pure calcium-containing stone component.

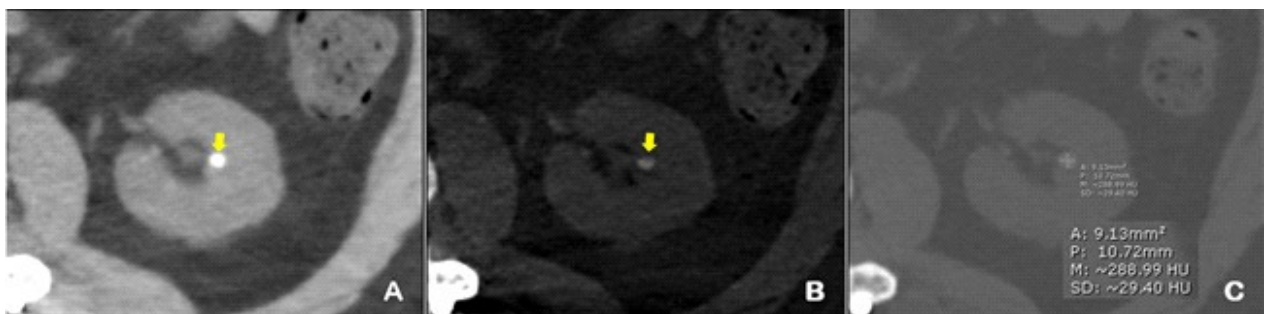


Figure 5. MD, water (A) and iodine (B), and NECT images (C) of a false negative stone. MD images showed a non-uric acid stone in left renal calyx. IRS revealed a pure uric acid component. The stone density measured on conventional 120 kVp NECT images was about 289 Hounsfield unit (HU), suggestive of uric acid component.^(5, 6, 14)

Table 1. Diagnostic accuracy of MD images compared to IRS.

	Value (%)	95% Confidence interval (%)
Sensitivity	50.0	1.3 - 98.7
Specificity	96.8	84.2 - 99.9
Positive predictive value (PPV)	50.0	1.3 - 98.7
Negative predictive value (NPV)	96.8	84.2 - 99.9
Accuracy	94.3	80.8 - 99.3

Discussion

The high specificity (96.8%), NPV (96.8%) and accuracy (94.3%) of MD images implied its benefit in non-uric acid stone determination.

There was a false positive determination of a uric acid stone from DECT (Figure 3), in which MD images showed the majority of uric acid component with minor lamellated non-uric acid component while the IRS result showed a majority of non-uric acid (Dahllite) component. A large band of streak artifact from pelvic bone across nearly entire this stone was found.

There was also a false negative determination of a non-uric acid stone (Figure 5), in which MD images showed a non-uric acid stone while the IRS result showed a pure uric acid component. However, this stone had an attenuation of about 289 HU on 120 kVp NECT images which was the attenuation of the uric acid stone.^(5, 6, 14) So, the determination of uric acid stone is better based on a combination of the attenuation on 120 kVp NECT images and MD images.

One uric acid stone in this study had been confirmed on both MD images and IRS. However, this stone was radio-opaque on a plain KUB radiograph (Figure 2). On MD images, although the majority of the stones (central part) showed uric acid component, thin peripheral high density on both water and iodine images was also present along with the stone attenuation about 590 HU on 120 kVp NECT images meaning that there should be some degree of non-uric acid component.^(5, 6, 14) These could explain why it was radio-opaque on a plain KUB radiograph. The IRS result of a pure uric acid stone might be due to sampling error because only some stone fragmentations obtained from percutaneous nephrolithotomy (PCNL) were sent for IRS.

Even though the prospective study design strengthened in avoidance of selection and recall biases, there were some limitations. First, there was a small number of included stones, especially uric

acid stones, despite over two years of data collection. Many patients had multiple stones but their locations were not labeled after the surgical extraction. Thus, the subsequent IRS results cannot be exactly matched to the stones seen on CT images. Moreover, stones that spontaneously passed or were treated with extracorporeal shock wave lithotripsy (ESWL) were unable to be collected. Second, this study simply divided the stones into two categories (uric and non-uric acid stones); in clinical practice, however, some stones may have more than one composition.

Conclusion

MD images from rapid-kV switching DECT can accurately determine non-uric acid urinary tract stones and offer high accuracy, specificity and NPV. However, the stone attenuation measured on conventional NECT still plays a role in uric acid and non-uric acid stone differentiation when the DECT is unavailable.

Conflict of interest

The authors have no conflict of interest to disclose.

References

1. Liu Y, Chen Y, Liao B, Luo D, Wang K, Li H, Zeng G. Epidemiology of urolithiasis in Asia. *Asian J Urol* 2018;5:205-14.
2. Sorokin I, Mamoulakis C, Miyazawa K, Rodgers A, Talati J, Lotan Y. Epidemiology of stone disease across the world. *World J Urol* 2017;35:1301-20.
3. Tosukhowonga P, Boonlaa C, Ratchanon S, Tanthanuch M, Poonpirome K, Supataravanich P. Crystalline composition and etiologic factors of kidney stone in Thailand: update 2007. *Asian Biomedicine* 2007;1:87-95.
4. Türk C, Skolarikos A, Neisius A, Petrik A, Seitz C, Thomas K. EAU guidelines on urolithiasis. *European Association of Urology* [Internet]. 2020 [cited 25 July 2020]. Available from: <https://uroweb.org/guideline/urolithiasis/>.

5. Kambadakone AR, Eisner BH, Catalano OA, Sahani DV. new and evolving concepts in the imaging and management of urolithiasis: urologists' perspective. *Radio Graphics* 2010;30:603–23.
6. Kulkarni NM, Eisner BH, Pinho DF, Joshi M, Kambadakone AR, Sahani DV Determination of renal stone composition in phantom. *J Comput Assist Tomogr* 2013;37:37-45.
7. Kaza RK, Ananthkrishnan L, Kambadakone A, Platt JF. Update of dual-energy CT applications in the genitourinary tract. *AJR Am J Roentgenol* 2017;208: 1185-92.
8. Rompsaithong U, Jongjitaree K, Korpraphong P, Woranisarakul V, Taweemonkongsap T, Nualyong C, Chotikawanich E. Characterization of renal stone composition by using fast kilovoltage switching dual-energy computed tomography compared to laboratory stone analysis: a pilot study. *Abdom Radiol (NY)* 2019;44:1027-32.
9. Kordbacheh H, Baliyan V, Singh P, Eisner BH, Sahani DV, Kambadakone AR. Rapid kVp switching dual-energy CT in the assessment of urolithiasis in patients with large body habitus: preliminary observations on image quality and stone characterization. *Abdom Radiol (NY)*. 2019;44:1019-26.
10. McGrath TA, Frank RA, Schieda N, Blew B, Salameh JP, Bossuyt PMM, McInnes MDF. Diagnostic accuracy of dual-energy computed tomography (DECT) to differentiate uric acid from non-uric acid calculi: systematic review and meta-analysis. *Eur Radiol* 2020;30:2791-801.
11. Marin D, Boll DT, Mileto A, Nelson RC. State of the art: dual-energy CT of the abdomen. *Radiology* 2014; 217:327-42.
12. Kravdal G, Helgø D, Moe MK. Infrared spectroscopy is the gold standard for kidney stone analysis. *Tidsskr Nor Lægeforen* 2015;135:313-4.
13. Cloutier J, Villa L, Traxer O, Daudon M. Kidney stone analysis: “Give me your stone, I will tell you who you are!”. *World J Urol* 2015;33:157-69.
14. Gucuk A, Uyeturk U. Usefulness of hounsfield unit and density in the assessment and treatment of urinary stones. *World J Nephrol* 2014;3:282-6.